The high-pressure, high-temperature phase diagram of cerium

The High-Pressure High-Temperature Phase Diagram of Cerium

K.A. Munro[1], D. Daisenberger[2], S.G. MacLeod[1 3 4], S. McGuire[3], I. Loa[1], C.A. Popescu[5], P. Botella[6 7], D. Errandonea[7], M.I. McMahon[1 4 *]

[1]SUPA, School of Physics and Astronomy and Centre for Science at Extreme Conditions, The University of Edinburgh, Peter Guthrie Tait Road, Edinburgh, EH9 3FD, UK

[2]Diamond Light Source Ltd., Harwell Science and Innovation Campus, Fermi Ave, Didcot, OX11 0DE, UK

[3]Atomic Weapons Establishment, Aldermaston, Reading, RG7 4PR, UK

[4]Research Complex at Harwell, Rutherford Appleton Laboratory, Harwell Oxford, Didcot, OX11 0FA, UK

[5]CELLS-ALBA Synchrotron Light Facility, Cerdanyola del Valles, 08290 Barcelona, Spain

[6]Division of Materials Science, Department of Engineering Science and Mathematics, Luleå University of Technology, 971 87 Luleå, Sweden

[7]Departamento de Física Aplicada-ICMUV, MALTA Consolider Team, Fundació General de la Universitat de València, Edificio de Investigación, c/Dr. Moliner 50, 46100 Burjassot, Valencia, Spain

E-mail: `m.i.mcmahon@ed.ac.uk`

Abstract.

We present an experimental study of the high-pressure, high-temperature behaviour of cerium up to ∼22 GPa and 820 K using angle-dispersive x-ray diffraction and external resistive heating. Studies above 820 K were prevented by chemical reactions between the samples and the diamond anvils of the pressure cells. We unambiguously measure the stability region of the orthorhombic $oC4$ phase and find it reaches its apex at 7.1 GPa and 650 K. We locate the α-$cF4$ – $oC4$ – $tI2$ triple point at 6.1 GPa and 640 K, 1 GPa below the location of the apex of the $oC4$ phase, and 1-2 GPa lower than previously reported. We find the α-$cF4 \rightarrow tI2$ phase boundary to have a positive gradient of 280 K/GPa, less steep than the 670 K/GPa reported previously, and find the $oC4 \rightarrow tI2$ phase boundary to lie at higher temperatures than previously found. We also find variations as large as 2-3 GPa in the transition pressures at which the $oC4 \rightarrow tI2$ transition takes place at a given temperature, the reasons for which remain unclear. Finally, we find no evidence that the α-$cF4 \rightarrow tI2$ is not second order at all temperatures up to 820 K.

Submitted to: *J. Phys.: Condens. Matter*

1. Introduction

Cerium (Ce) has long been the focus of both computational and experimental studies of $4f$ electron behaviour, and is a perfect example of an element displaying a pressure-induced electronic transition [1]. Ce crystallises in either the γ phase (with the fcc structure, denoted $cF4$ in Pearson notation), or the β phase (with the dhcp structure denoted $hP4$ in Pearson notation) at ambient conditions [2]. Single-phase $hP4$ can be made by thermally cycling Ce between room temperature (RT) and 4 K followed by annealing for long periods at 348 K [3].

Ce is best known for its pressure-induced isostructural transition from the γ phase to the α phase (also $cF4$) at 0.7 GPa and RT, which is accompanied by a large decrease in volume [2]. Since both the γ and α phase have the same structure they will be referred to as γ-$cF4$ and α-$cF4$ hereafter. Uniquely in the elements, the γ-$cF4 \rightarrow \alpha$-$cF4$ phase line ends at a critical point [4], most recently estimated to be at 1.5 GPa and 480 K [5], as shown in Figure 1 [6], where Ce becomes a solid without compressive strength but with finite shear strength [7]. The mechanisms behind the γ-$cF4 \rightarrow \alpha$-$cF4$ transition have been intensely debated. The $4f$ electrons are key to the transition, but to what extent electron screening, electron de-localisation and vibrational energy drive this transition, and whether the transition is best described by the Mott Transition model [8] or the Kondo Volume Collapse (KVC) model [9] is still a subject of ongoing research (see [10], and the extensive review by Nikolaev and Tsvyashchenko [11], and the references therein).

Upon further compression at RT, Ce undergoes a phase transition, at $\sim$4 GPa. Early x-ray diffraction experiments reported that the transition is to a C-centered orthorhombic structure ($oC4$ in Pearson notation and denoted α' in the literature), isostructural with that found in α-uranium at ambient conditions [12, 13]. Subsequent x-ray studies [14, 15], however, concluded that Ce transforms to a C-centered monoclinic structure ($mC4$ in Pearson notation and denoted α'' in the literature), while others observed both the $oC4$ and $mC4$ structures [16, 17]. It was later shown that it was possible to transform α-$cF4$ into either the $mC4$ or the $oC4$ structure depending on the prior mechanical treatment of the sample [18]: samples cut from an ingot transform into the $oC4$ structure [16, 17, 19], while cold-worked samples or small shavings favour the $mC4$ structure [14, 15, 19].

Upon further compression at RT, both the $oC4$ and $mC4$ phases transform into a body centered tetragonal (bct) structure ($tI2$ in Pearson notation, and denoted ϵ in the literature) at $\sim$12 GPa, which remains stable up to 208 GPa [20], the highest pressure to which Ce has been studied.

There have been many theoretical and computational studies on the stability of the post α-$cF4$ phase, though different first-principle techniques (all performed at 0 K, and therefore considering the energetics of the static lattice) yield different results. The linear muffin-tin orbital (LMTO) model favours the $oC4$ structure [21, 22], while applying the full-potential linear muffin-tin orbital (FP-LMTO) model to the same problem finds

$mC4$ to be the only stable phase [23]. Later work using the FP-LMTO model combined with the generalised gradient approximation (GGA) reported that both $oC4$ and $mC4$ are meta-stable and α-$cF4$ transforms directly into the $tI2$ phase [24]. Local density approximations (LDA), or GGA calculations using the plane wave method + pseudo-potential confirmed the metastable nature of both phases [25]. However, when LDA is combined with the Gutzwiller variation approach the result is altered and the $mC4$ structure is the only stable solution [26]. Despite the large number of theoretical studies a consensus has therefore not been reached as to whether the ground state has the $oC4$ or $mC4$ structure.

There is also very little experimental consensus for which of the phases is the most stable between 5 and 12 GPa at RT. Zachariasen *et al.* [27] reported that upon pressure cycling their $oC4$+$mC4$ mixed-phase sample, it transformed into a pure $oC4$ phase, which suggested that slow rates of pressure change favour the $oC4$ phase. Zachariasen *et al.* also noted that the α-$cF4 \rightarrow mC4$ transition requires a very small shift in atomic positions, whereas the α-$cF4 \rightarrow oC4$ and $mC4 \rightarrow oC4$ transitions require more substantial atomic reorganisation. Most recently, Ma *et al.* have reported that they observed either the $oC4$ or $mC4$ phases, depending on whether or not the sample had been precompressed [28] (that is, loaded and then held at 1.5 GPa for three days before the rest of the experiment was performed), and that in the precompressed samples a small amount of the $mC4$ phase transformed into $oC4$ on further compression. Upon heating the $mC4$ phase, Zhao *et al.* reported that Ce transforms into the $oC4$ phase which remains stable on cooling back down to RT [17]. This is consistent with the results of Dmitriev *et al.* [29], who reported that while they observed the $mC4$ phase on compression at RT, compression of the α-$cF4$ phase at 473 K resulted in a transition to the $oC4$ phase.

There have also been a number of high-pressure, high-temperature studies of Ce with the aim of exploring the $oC4$+$mC4$ stability region [6, 17, 30, 31, 32]. The initial studies by King *et al.* [33] and Endo *et al.* [30] focused on the α-$cF4 \rightarrow mC4$ and $mC4 \rightarrow tI2$ phase boundaries, respectively, although King *et al.* presented no evidence that they observed the $mC4$ phase above 5 GPa rather than the $oC4$ phase. Both phase boundaries were found to have a negative slope, and were incorporated into a fuller phase diagram determined by Antonova *et al.* using differential thermal analysis (DTA) and resistivity techniques [31]. By collecting both isothermal and isobaric data, on both pressure and temperature increase and decrease, Antonova *et al.* established the α-$cF4 \rightarrow oC4$+$mC4$ phase boundary to be curved at high temperature with a large hysteresis between the transition pressures seen on compression and release (see Figure 1). By combining their own data with the $mC4 \rightarrow tI2$ phase boundary of Endo *et al.*, Antonova *et al.* suggested that the $oC4$+$mC4$ stability field was dome shaped, and that the α-$cF4$ – ($oC4$+$mC4$) – $tI2$ triple point was at 8.5 GPa and 630 K. Although they obtained no data on the α-$cF4 \rightarrow tI2$ phase boundary, they indicated the likely position and gradient of such a boundary.

Subsequent high-pressure high-temperature diffraction data obtained by Zhao *et*

al. [17] suggested that the $mC4$ phase irreversibly disappeared at temperatures above 400 K, and was generally consistent with the phase diagram proposed by Antonova *et al.* However, while the phase boundary between $oC4$+$mC4$ and $tI2$ was reported as linear, its slope was steeper than that originally reported by Endo *et al.* [30]. Zhao *et al.* also confirmed the location of the α-$cF4$ – ($oC4$+$mC4$) – $tI2$ triple point at 8.5 GPa and 625 K, but provided no new information on the nature of the α-$cF4 \rightarrow tI2$ phase boundary.

Tsiok *et al.* [32] performed an extensive high-pressure, high-temperature resistivity study to 15 GPa and 710 K. In contrast to previous studies, they concluded that the $tI2$ phase was only meta-stable, and that it transformed back to the α-$cF4$ phase above ∼673 K at pressures above 12 GPa (see Figure 1). They also reported that the structure assumed by Ce at any given pressure and temperature was highly dependent on the trajectory in $P-T$ space taken to get to that point. The subsequent diffraction study of Schiwek *et al.* [6], however, confirmed the general phase diagram reported by Zhao *et al.* and located the α-$cF4 \rightarrow tI2$ phase boundary, which was found to have a steep positive slope, and therefore to be almost perpendicular to that proposed by Tsiok *et al.*

Schiwek *et al.* also determined the α-$cF4$–$oC4$–$tI2$ triple point to be located around 6.9 GPa and 600 K, coinciding with the apex of the stability region of the $oC4$+$mC4$ phases which was reported as dome-shaped - see Figure 1 [6]. While the shape of this stability region is very similar to that originally proposed by Antonova *et al.*, the $oC4$+$mC4 \rightarrow tI2$ phase boundary is slightly different to that reported by Endo and Zhao.

Despite many studies, therefore, the phase diagram of Ce still appears to be uncertain. This is particularly true when phase boundary determinations were made without the identity of the phases concerned ($oC4$ or $mC4$) being determined unequivocally using x-ray diffraction.

This uncertainty is further highlighted by our own preliminary diffraction data obtained on isothermal compression at ∼650 K, which showed a α-$cF4 \rightarrow tI2 \rightarrow oC4 \rightarrow tI2$ transition sequence. This is incompatible with all previously published phase diagrams, and suggests (i) contrary to the report by Tsiok *et al.*, but in agreement with Endo, Zhao and Schiwek, that the $tI2$ phase is indeed found at high temperatures, and (ii) that the α-$cF4 \rightarrow tI2$ phase line intercepts the dome shaped $oC4$+$mC4$ stability region on the low-pressure side of its apex, contrary to that shown in Figure 1. To address these inconsistencies, and to make a definitive diffraction study of cerium's high-pressure, high-temperature phase diagram, we have performed angle-dispersive x-ray diffraction experiments using diamond anvil cells (DACs) and synchrotron radiation up to 20 GPa and 820 K.

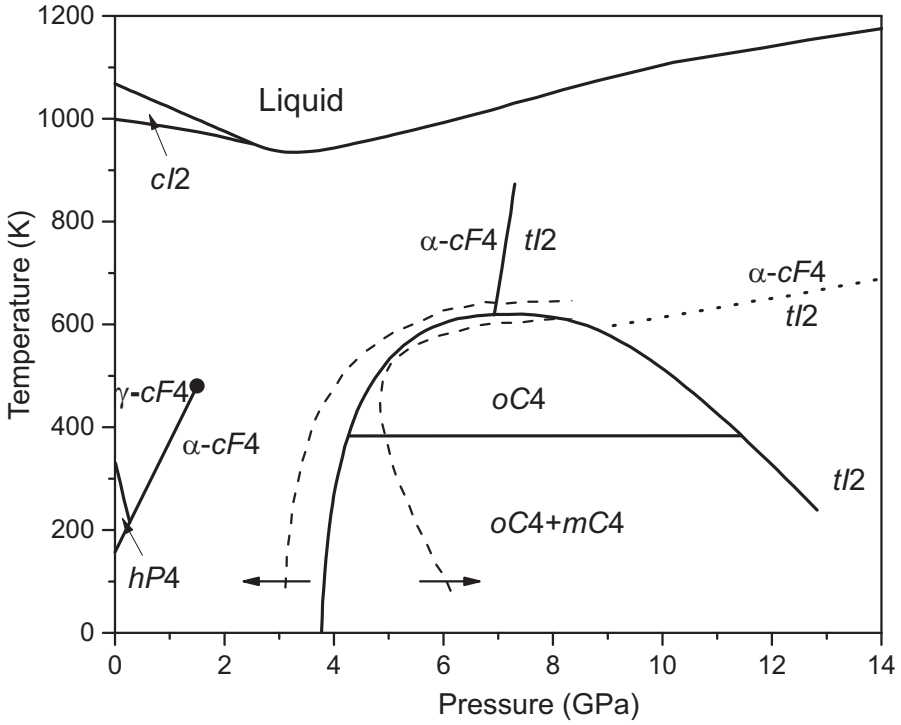

Figure 1. The phase diagram of Ce, based on the present literature, with the different phases identified using their Pearson notation. The phase boundaries shown with solid lines are those reported by Schiwek *et al.* [6], while the dashed lines show the forward and reverse transition pressures from and to the α-$cF4$ phase reported by Antonova *et al.* [31]. The dotted line shows the suggested phase line between the α-$cF4$ and $tI2$ phases reported by Tsiok *et al.* [32].

2. Experimental Details

All of the Ce samples used in this study were cut from a high purity (99.99+%) Ce ingot, provided by U. Schwarz of the MPI für Chemische Physik fester Stoffe in Dresden. As the $mC4$ phase is reported to irreversibly disappear above 400 K [17], we prepared our samples such that the $oC4$ phase would be observed at RT, thereby ensuring that the α-$cF4 \rightarrow oC4$ and $oC4 \rightarrow tI2$ transitions were studied at all temperatures. The samples were therefore cut using sharp scalpel blades in an oxygen-free, water-free glovebox environment (<1 ppm O_2 and <1 ppm H_2O), taking care to minimise the mechanical deformation of the sample which induces the transition to the $mC4$ phase [18].

For RT experiments, the Ce samples were loaded into Merrill-Bassett (MB) DACs equipped with tungsten gaskets, and loaded with a small piece of 1 μm thick Ta foil or a small sphere of Cu as a pressure marker. The cells were loaded and sealed in the same oxygen-free, water-free environment used to prepare the samples. No pressure transmitting medium was included to prevent sample contamination, and to minimise any chemical reactions occurring within the sample chamber during sample loading.

The samples studied in the high-pressure, high-temperature experiments were

prepared as described above. Samples were loaded into membrane DACs equipped with rhenium gaskets, which were then placed into a custom-built vacuum vessel [34, 35]. The samples were heated with Watlow 240 V coiled heaters, which were wrapped around the outside of the DACs. The temperature was measured by using a K-type thermocouple attached to one of the diamond anvils, close to the gasket. Various pressure markers were used in the high-temperature experiments. Ta, Cu and NaCl were used as pressure markers, with the pressure being determined using the thermal equations of state (EoS) of Dorogokupets *et al.* [36], Cynn *et al.* [37] and Dorogokupets *et al.* [38], respectively.

The majority of the x-ray diffraction data used in this study was collected from multiple experiments on the high-pressure beamline I15 at the Diamond Light Source using a monochromated x-ray beam with incident wavelengths of ∼0.4246 Å or 0.3113 Å, collimated to 20 μm in diameter, and a MAR345 area detector. However, other diffraction data were also collected on beamline BL04 at the ALBA synchrotron and on beamline ID09a at the ESRF synchrotron using similar x-ray wavelengths and beamsizes. In total, over 1600 diffraction images were collected from 13 samples in 6 separate synchrotron visits. In all experiments the 2-D diffraction images were integrated azimuthally using Fit2D [39] and analysed using Le Bail profile fitting with the Jana software [40]. Apart from the DACs loaded with NaCl, no pressure transmitting medium was included with the sample. As a result, the samples may have experienced non-hydrostatic pressure. The methods of Singh *et al.* were utilized to quantify any non-hydrostatic effects in the $cF4$ phases [41] and, despite not using a pressure transmitting medium, no non-hydrostatic effects were observed. In addition, no systematic misfits between the observed and calculated peak positions were observed in the $oC4$ and $tI2$ phases, suggesting that non-hydrostatic effects were undetectable.

3. Results

3.1. Room-Temperature Compression

We performed two RT compression experiments. The two samples were compressed at RT up to 21.8 GPa, one using Ta as the pressure marker, while the other used Cu. After the DACs were closed in the glovebox, the samples were found to be in either the hexagonal $hP4$ phase, or in the γ-$cF4$ phase, depending on the pressure in the DACs. At low pressures, mixed-phase $hP4/\gamma$-$cF4$ diffraction profiles were observed, with single-phase γ-$cF4$ profiles being obtained only above 1.0 GPa. The onset of the γ-$cF4 \rightarrow \alpha$-$cF4$ isostructural transition was observed at 1.1 GPa in both samples, and by 1.8 GPa no trace of γ-$cF4$ remained.

Regions of the 2-D diffraction images obtained from the Ta-containing DAC on compression up to 21.8 GPa are shown in Figure 2, and a selection of integrated profiles is shown in Figure 3. As the pressure was increased, multiple Bragg spots appeared in the raw 2-D images at 4-5 GPa (Figure 2(b)), indicating the growth of a single crystal which is characteristic of a transition to the $oC4$ structure [18, 16]. Le Bail fitting

techniques were used to confirm the identity of the $oC4$ phase. The cell containing the Ta marker indicated the transition started at 4.0(1) GPa, while the Cu-containing DAC showed that the transformation started at 5.2(3) GPa. These transition pressures are in good agreement with previously reported values [16, 17, 27].

As the pressure was increased further, the diffraction images from the $oC4$ phase gradually became less single-crystal-like and more powder-like (Figure 2(c)). The phase transition to the $tI2$ phase near 12 GPa was identified by the appearance of the (110) peak from this phase (Figure 2(d)), and diffraction images from $tI2$ comprised textured Deybe-Scherrer rings, with non-uniform intensities around the rings (see Figure 2(d) & (e)). The $oC4 \rightarrow tI2$ transition occurred at 12.4(2) GPa in the Ta-containing DAC, and at 12.6(2) GPa in the Cu-containing DAC, both in good agreement with previous reports [14, 29].

We observed a wide range of co-existence of the $oC4$ and $tI2$ phases at RT, such that single-phase diffraction patterns from the $tI2$ phase were observed only above 21.8 GPa (Figure 3). A large co-existence range of these phases has been reported previously - between 13 and 19 GPa by Gu *et al.* [16], and between 13.3 and 17.6 GPa by Ma *et al.* [42]. We believe that the larger co-existence range observed in the current study arises because of the single-crystal like nature of our $oC4$ samples. This resulted in extremely intense reflections from the $oC4$ phase such that we could still see evidence of the $oC4$ reflections at higher pressures (21 GPa) than if we had a more powder-like sample. Indeed, it was *only* in the 2D images that we could see evidence of the very weak peaks from the $oC4$ phase at 21 GPa; the integrated profiles showed no evidence above 19.0 GPa, in better agreement with previous studies.

The extended co-existence range of the $oC4$ and $tI2$ phases at RT may arise from their very different crystal structures, as a transition between the two requires considerable atomic rearrangement. However, Endo *et al.* [14] and Dmitriev *et al.* [29] both reported co-existence of the monoclinic $mC4$ phase and the $tI2$ phase between 12.1 and 17.5 GPa, and 12.5 and 17.7 GP, respectively, at 300 K. These ranges are similar to those reported for the $oC4$ and $tI2$ phases (see above), yet both the $mC4$ and $tI2$ structures are only slightly distorted from fcc, and little atomic rearrangement is required to transform between them. The structural changes required at the transition would not therefore seem to be the main reason behind the large co-existence region, and further understanding is needed.

3.2. Resistive-Heating Studies

We used the resistively-heated DACs to determine the phase boundaries between the α-$cF4$, $oC4$ and $tI2$ phases up to ∼820 K and 20 GPa. As expected from the sample-preparation method used, we observe no evidence of the monoclinic $mC4$ phase in any sample, thus enabling us to locate phase transitions to and from the $oC4$ phase unambiguously. After loading, the samples were initially compressed into the α-$cF4$ phase at ∼3 GPa and then heated to the required temperature. They were then

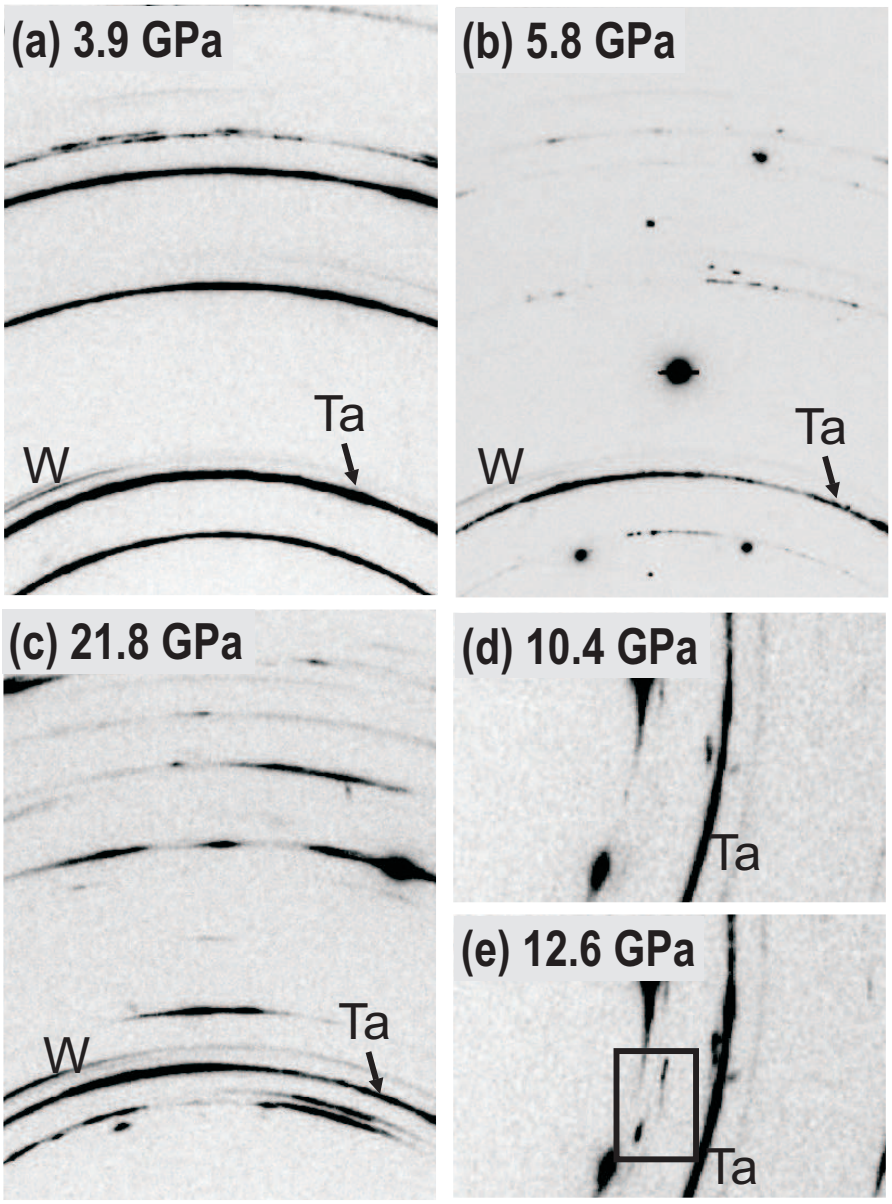

Figure 2. 2-D diffraction images of Ce obtained on compression at RT. (a) The α-$cF4$ phase at 3.9 GPa, (b) the $oC4$ phase at 5.8 GPa, and (c) the $tI2$ phase at 21.8 GPa. Debye-Scherrer (D-S) rings from the Ta pressure marker and the W gasket are labeled. The transition to the $oC4$ phase is marked by the appearance of intense Bragg spots as the initially polycrystalline sample becomes single-crystal like (compare (a) and (b)), while the D-S rings from the $tI2$ phase are highly textured (panel (c)). Panels (d) and (e), obtained at 10.4 and 12.6 GPa, respectively, highlight the appearance of low-angle reflections that mark the onset of the $oC4 \rightarrow tI2$ phase transition.

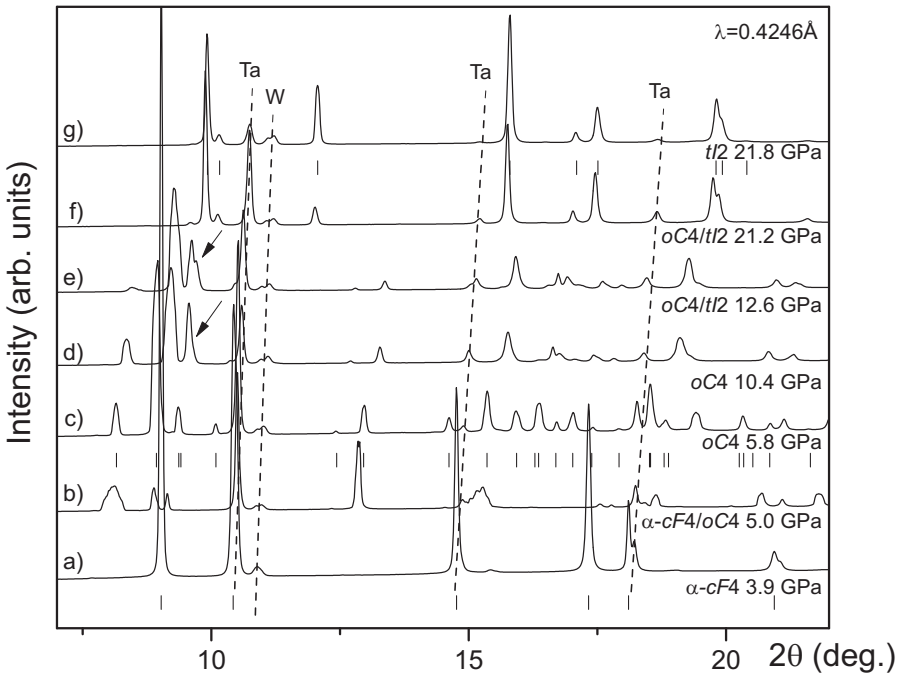

Figure 3. Integrated x-ray diffraction profiles obtained from Ce on compression at RT. Peaks arising from the Ta pressure marker and the W gasket are labeled, while the tick marks beneath the single-phase (a) α-$cF4$, (c) $oC4$ and (g) $tI2$ profiles at 3.9, 5.8 and 21.8 GPa, respectively, show the expected peak positions in these three phases. The shapes of some of the peaks from the $oC4$ phase in profiles (b) and (c) are unusual due to the single-crystal nature of the reflections in the respective 2D images.

compressed isothermally until single-phase $tI2$ diffraction patterns were obtained. We also attempted to study the $oC4 \rightarrow \alpha$-$cF4$ and $tI2 \rightarrow oC4$ reverse phase transitions on decompression, but the piston-cylinder DACs used in this study have a tendency to seize at high temperatures, making controlled pressure release very difficult. Each isothermal compression was therefore obtained with a different sample. However, in one case, the DAC remained loose enough to enable us to repeatedly compress and decompress the cell. The sample in this DAC was therefore used to study the α-$cF4 \leftrightarrow tI2$ phase boundary, with data being collected on both compression and decompression.

Figure 4 shows the phase boundaries that best fit our experimental data. We note that there is some scatter in the transition pressures observed for the $oC4 \rightarrow tI2$ transitions above 10 GPa, and we return to this later. The α-$cF4 \rightarrow oC4$ phase boundary lies within the region of hysteresis observed by Antonova *et al.* [31]. However, the detailed shape of the $oC4$ stability region at higher pressures is different to what has been reported previously, reaching an apex at ∼7.1 GPa and ∼650 K after which the $oC4 \rightarrow tI2$ phase boundary becomes negatively sloped, and increasingly so above ∼11 GPa. We locate the triple point between the α-$cF4$, $oC4$ and $tI2$ phases at 6.1 GPa and 640 K, some 1-2 GPa lower than previous estimates, and find the α-$cF4 \rightarrow tI2$ boundary to have a positive gradient less steep (∼280 K/GPa versus ∼670 K/GPa)

than previously estimated.

Attempts to follow the α-$cF4 \rightarrow tI2$ phase boundary up to the melting line above 1000 K were unsuccessful. Above ∼550 K weak additional contaminant peaks appeared in the diffraction profiles (as highlighted in Figure 5) and above 820 K stronger non-Ce peaks appeared in the diffraction patterns signifying a reaction of the sample with either the gasket or the diamond anvil. The strength of the contaminant peaks suggests that less than 1% of the Ce sample has reacted when they first appear above 550 K, and that this increases to ∼1% at 770 K and ∼10% at 820 K. At 880 K the contaminant peaks dominated the diffraction profile, such that no further analysis of the Ce sample was possible. Analysis of the pressure cell after disassembly showed that the culets of both anvils were deeply pitted exactly where the sample had been in contact with them. The hot Ce had therefore reacted with the diamonds above 820 K, and studies to higher temperatures will require that the anvils are protected from the Ce by a chemical barrier. There remains a question as to how the presence of the contaminant phase affected studies of the transition pressures across the α-$cF4 \rightarrow tI2$ phase boundary. As said, up to 820 K, a maximum of 10% of the sample had reacted, and the diffraction peaks from the Ce sample remained clearly visible. The reactant was likely to be concentrated in two layers adjacent to the anvil culets with the unreacted sample present in the middle of the gasket hole. As this is the same sample geometry that one would have if the Ce were sandwiched between two layers of a pressure transmitting medium, we believe the presence of the contaminant up to 820 K had no effect on the measurements presented here.

Schiwek *et al.* [6] reported that the α-$cF4 \rightarrow tI2$ phase boundary intercepts the $oC4$ stability field at its apex. Our data, and the requirement of an α-$cF4 \rightarrow tI2 \rightarrow oC4 \rightarrow tI2$ phase transition sequence on isothermal compression at ∼650 K seen in our preliminary study, reveal that the α-$cF4 \rightarrow tI2$ phase boundary intercepts the $oC4$ stability field at lower pressures and temperatures than the position of the apex. Analysis of the diffraction patterns obtained across the α-$cF4 \rightarrow tI2$ transition shows a sharp onset of the $tI2$ phase (as determined by the splitting of the diffraction peaks from α-$cF4$), with no observable hysteresis (see Figure 5) nor co-existence of the two phases. We also see no volume discontinuity, and there is therefore no evidence that the α-$cF4 \rightarrow tI2$ is not second order.

Following the analysis of Schiwek *et al.* and Zhao *et al.*, the c/a ratio of $tI2$ was plotted against V/V_0 to determine whether or not the α-$cF4 \rightarrow tI2$ transition is continuous. Figure 6 shows the tetragonal distortion of the $tI2$ phase (denoted $c/a - \sqrt{2}$) plotted against the reduced volume (V/V_0) on both pressure increase (filled symbols) and decrease (unfilled symbols) as a function of temperature. The distortion is zero in the α-$cF4$ phase. There is no evidence of systematic hysteresis in the transition pressure or c/a ratio on pressure increase and decrease. There is also no evidence of any discontinuity in c/a at the α-$cF4 \rightarrow tI2$ transition at any temperature other than 643 K, where two data points, one collected on pressure increase (at V/V_0=0.7078) and the other on pressure decrease (at V/V_0=0.7075) may suggest a discontinuity. However, as

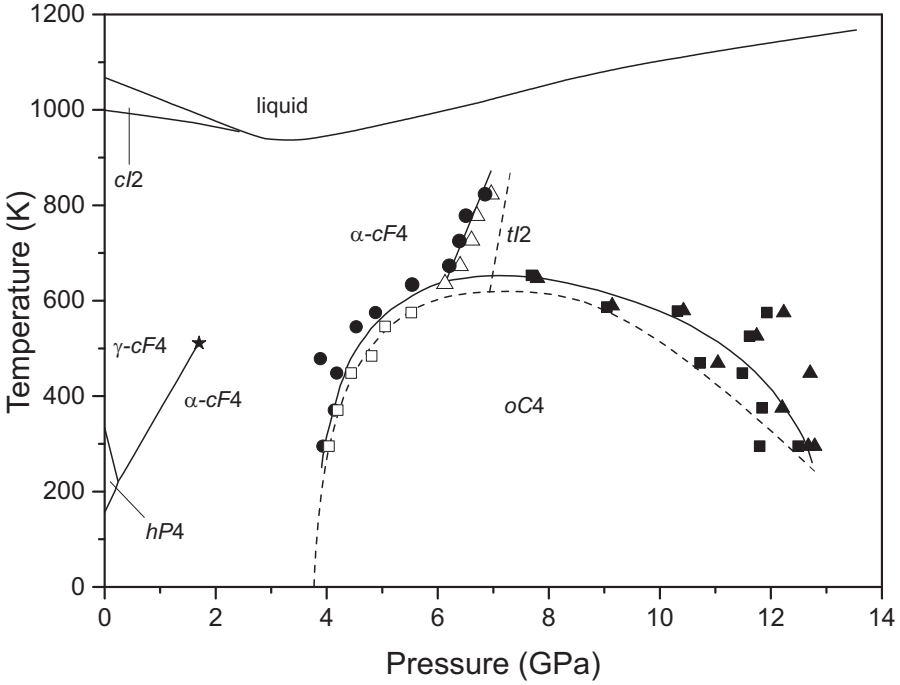

Figure 4. The proposed P-T phase diagram of Ce. The data were collected along a series of isotherms, and the filled circles mark the highest pressure at which single-phase α-$cF4$ diffraction patterns were observed at each temperature, while the unfilled squares and triangles immediately to their right show the pressures at which the $oC4$ and $tI2$ phases, respectively, were first observed on compressing the same samples. Similarly, at higher pressures, the filled squares mark the highest pressure at which single-phase $oC4$ diffraction patterns were observed, while the filled triangles to their right show the pressures at which the $tI2$ phase was first observed in the same samples. The dashed lines show the phase boundaries reported by Schiwek *et al.* [6], and references therein, while the solid lines show the phase boundaries that best-fit the current data.

it is unlikely that the order of the transition is different at only one temperature, we believe that the apparent discontinuity at 643 K arises from the scatter in the two data points.

The experimental evidence, therefore, is that the α-$cF4 \rightarrow tI2$ transition is continuous up to 800 K. While Figure 6 suggests that the tetragonal distortion is temperature dependent at a fixed volume, this effect arises from the finite slope of the α-$cF4 \rightarrow tI2$ phase boundary (see Figure 4), such that along an isochore (for example V/V_0 =0.705 in Figure 6) the sample is closer to the phase boundary at higher temperatures, resulting in a smaller tetragonal distortion of the $tI2$ phase. Indeed, at V/V_0 =0.705, one can estimate the tetragonal distortion from the data shown at six different temperatures in Figure 6 and determine that the distortion decreases linearly with temperature. At V/V_0 =0.705, the tetragonal distortion reduces to 0 at ∼825 K, and the α-$cF4 \rightarrow tI2$ transition would therefore take place at this compression and temperature, in agreement with the α-$cF4 \rightarrow tI2$ phase boundary shown in Figure 4.

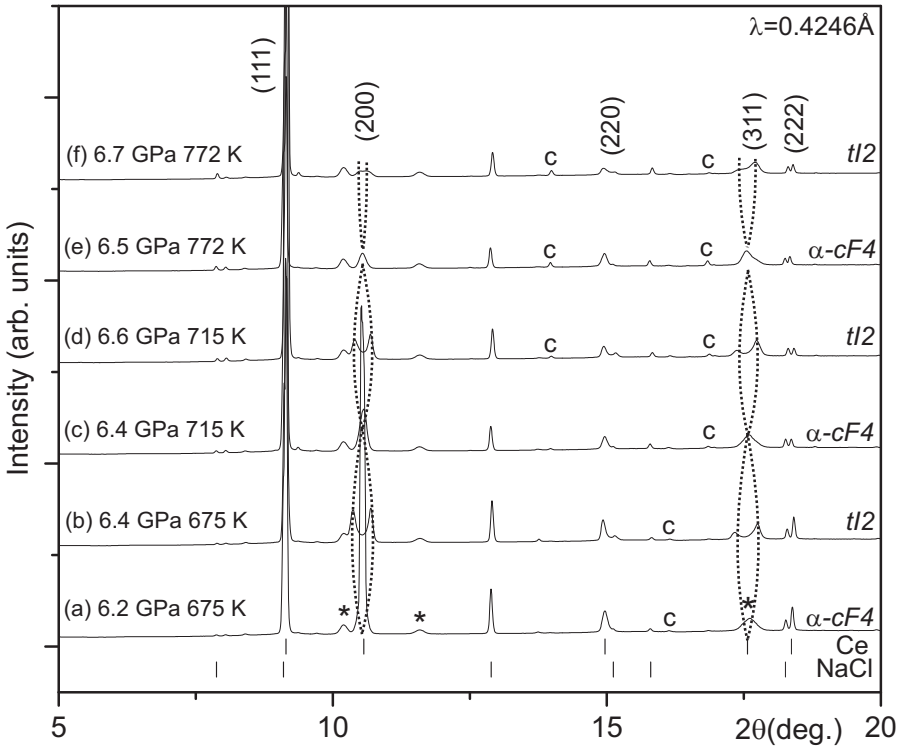

Figure 5. Ce diffraction profiles showing the transition from α-$cF4$ to $tI2$ structure on pressure increase at 675 K (profiles (a) and (b)), 715 K (profiles (c) and (d)), and 772 K (profiles (e) and (f)).The bowed dotted lines highlight the splitting of the (200) and (311) peaks from α-$cF4$ into the (002)/(110), and (103)/(211) doublets, respectively, in the $tI2$ phase. The asterisks in profile (a) mark weak peaks from the rhenium gasket. Other weak peaks marked 'c' come from the contaminant phase which appeared at elevated temperatures.

Finally, we return to the relatively large scatter seen in the transition pressures and temperatures above 10 GPa (Figure 4). Tsoik *et al.* reported that the structures assumed by Ce at any given P and T were highly dependent on the P-T path taken to get to that point in phase space [32]. As mentioned earlier, all of the diffraction data presented in this study were obtained on isothermal compression, and, with the exception of the data used to determine the α-$cF4 \rightarrow tI2$ phase boundary, each isotherm was obtained with a different sample. The compression paths followed to obtain data at each P-T point were therefore as simple as they could be. Also, by using x-ray diffraction, we were able to identify unambiguously the structures involved in the phase transitions, thereby ruling out that the scatter arose from transitions between different structures at each temperature (for example $mC4 \rightarrow tI2$ rather than $oC4 \rightarrow tI2$). Despite this, we see substantial variations in the pressure at which the $oC4 \rightarrow tI2$ transition was observed at each temperature. For example, we found variations of $\sim$3 GPa in the $oC4 \rightarrow tI2$ phase transition pressure in multiple measurements made at $\sim$575 K (see Figure 4). The reasons for this significant variation are unclear. The different samples were from the same source, prepared in the same manner, and were loaded with the

same pressure marker. We can therefore rule out variations in the transition pressure as arising from sample or pressure calibration issues. And while the first-order nature of the $oC4 \rightarrow tI2$ transition may result in variations in the transition pressure at lower temperatures, one might expect such variations to be reduced at elevated temperatures such as 575 K. Further studies of the $oC4 \rightarrow tI2$ transition are required.

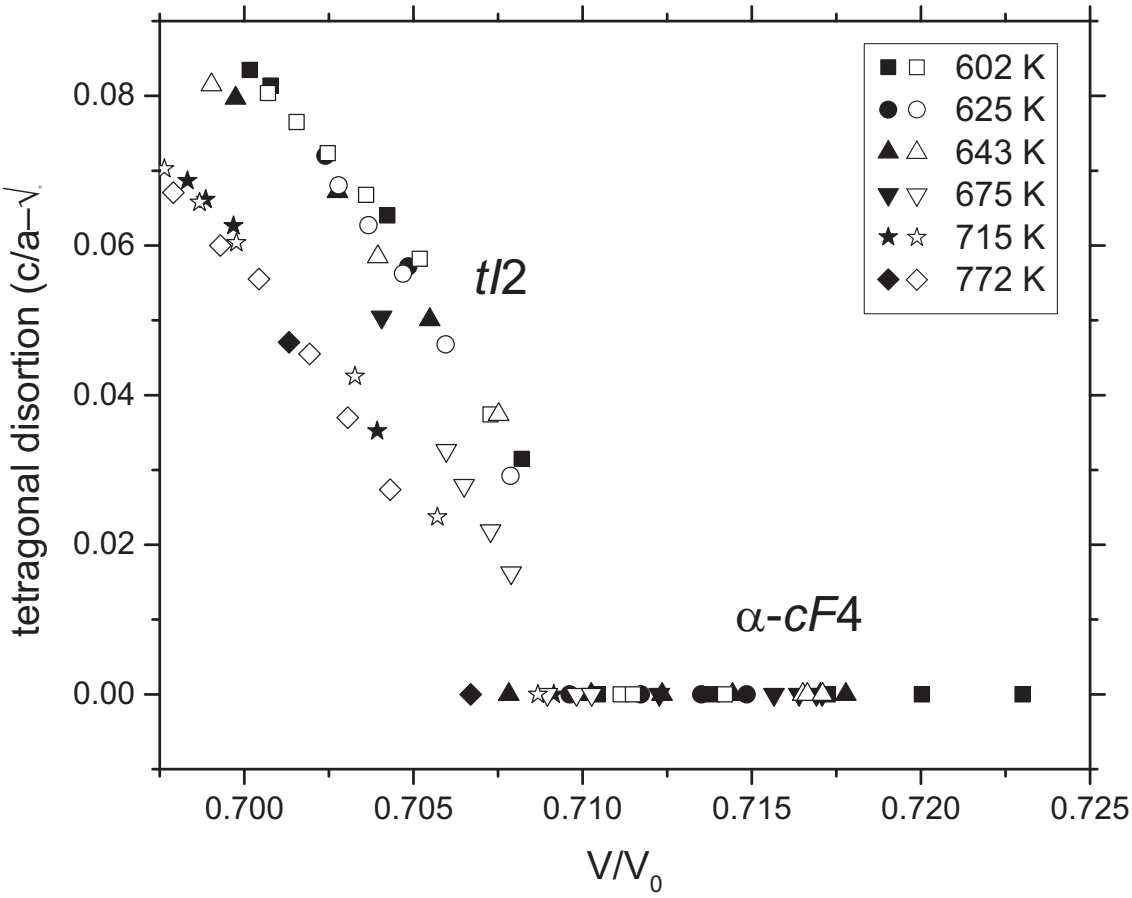

Figure 6. The tetragonal distortion of the $tI2$ (defined as $c/a-\sqrt{2}$) and α-$cF4$ phases of Ce plotted against V/V_0 along various isotherms. Data collected on pressure increase/decrease at each temperature are denoted with filled/hollow symbols.

4. Conclusions

Angle dispersive x-ray powder diffraction experiments have been performed on Ce up to 22 GPa and 820 K, with the aim of determining the stability region of the $oC4$ phase, and nature of the α-$cF4 \rightarrow tI2$ phase boundary. The low-pressure phase boundary between the α-$cF4$ and $oC4$ phases is in good agreement with previous studies. The triple point between the α-$cF4$, $oC4$ and $tI2$ is found at 6.1 GPa and 640 K, 1-2 GPa lower than previous estimates, and is not at the apex of the $oC4$ phase stability region, which is located at 7.1 GPa and 650 K. The α-$cF4 \rightarrow tI2$ phase boundary is found to have a positive gradient less steep ($\sim$ 280 K/GPa versus $\sim$ 670 K/GPa) than previously

estimated. We find the α-$cF4 \rightarrow tI2$ transition to be second order, in contrast to the conclusions reported by Zhao *et al.* [17].

Our data suggest that the $oC4 \rightarrow tI2$ phase boundary lies at higher temperatures than reported previously, and we observe significant scatter in the phase transition pressures observed at any given temperature, the reasons for which are unclear and require further study. In contrast to the claims of Tsiok *et al.* [32], we observed no evidence of the α-$cF4$ at pressures above the triple point, only the $tI2$ phase.

Unfortunately, we were unable to study Ce above 820 K due to reactions between the Ce and the diamond anvils. The location of the α-$cF4-tI2-$liquid triple point thus remains unknown, while the phase behaviour at higher pressures and temperatures remains completely unknown. Given the reaction observed between the Ce and the diamond anvils above 820 K, further studies to investigate the higher pressure/temperature behaviour will need to ensure that the Ce is contained within a non-reactive pressure medium and prevented from contacting the anvils.

5. Acknowledgments

K.A.M. thanks the UK Engineering and Physical Sciences Research Council (EPSRC) and AWE for financial support. M.I.M. is grateful to AWE for the award of a William Penney Fellowship. ©British Crown Owned Copyright 2019/AWE. Published with permission of the Controller of Her Britannic Majesty's Stationary Office. This work was supported by Grant No. EP/R02927X/1 from the EPSRC and facilities made available by the Diamond Light Source. D.E. acknowledges the financial support from the Spanish Ministerio de Ciencia, Innovación y Universidades, the Spanish Research Agency, the Generalitat Valenciana, and the European Fund for Regional Development under Grants No. MAT2016-75586-C4-1-P, PGC2018-097520-A-100, and Prometeo/2018/123 (EFIMAT). We express our gratitude to U. Schwarz of the MPI für Chemische Physik in Dresden for providing the high-purity samples of Ce.

6. References

[1] Samudrala G K and Vohra Y K 2013 Structural properties of lanthanides at ultra high pressure (*Handbook on the Physics and Chemistry of Rare Earths* vol 43) (Elsevier) pp 275 – 319

[2] Lawson A W and Tang T Y 1949 *Phys. Rev.* **76**(2) 301–302

[3] Koskimaki D C, Gschneidner K A and Panousis N T 1974 *Journal of Crystal Growth* **22** 225 – 229

[4] Jayaraman A 1965 *Phys. Rev.* **137**(1A) A179–A182

[5] Lipp M J, Jackson D, Cynn H, Aracne C, Evans W J and McMahan A K 2008 *Phys. Rev. Lett.* **101**(16) 165703 URL `https://link.aps.org/doi/10.1103/PhysRevLett.101.165703`

[6] Schiwek A, Porsch F and Holzapfel W B 2002 *High Press. Res.* **22** 407–410

[7] Lipp M J, Jenei Z, Cynn H, Kono Y, Park C, Kenney-Benson C and Evans W J 2017 *Nature Communications* **8** 1198 ISSN 2041-1723 URL `https://doi.org/10.1038/s41467-017-01411-9`

[8] Johansson B 1974 *Philosophical Magazine* **30** 469–482

[9] Allen J W and Martin R M 1982 *Phys. Rev. Lett.* **49**(15) 1106–1110

[10] Lu H and Huang L 2018 *Journal of Physics: Condensed Matter* **30** 395601 ISSN 1361-648X URL http://dx.doi.org/10.1088/1361-648X/aadc7c
[11] Nikolaev A V and Tsvyashchenko A V 2012 *Sov. Phys. Usp* **55** 657
[12] Ellinger F H and Zachariasen W H 1974 *Phys. Rev. Lett.* **32**(14) 773–774
[13] Bocquillon G, Epain R and Loriers C 1978 *J. Appl. Phys.* **49** 4431–4432
[14] Endo S, Sasaki H and Mitsui T 1977 *J. Phys. Soc. JPN* **42** 882–885
[15] Olsen J, Gerward L, Benedict U and Itié J P 1985 *Phys. B+C* **133** 129 – 137
[16] Gu G, Vohra Y K and Brister K E 1995 *Phys. Rev. B* **52**(13) 9107–9110
[17] Zhao Y and Holzapfel W 1997 *Journal of Alloys and Compounds* **246** 216 – 219
[18] McMahon M I and Nelmes R J 1997 *Phys. Rev. Lett.* **78**(20) 3884–3887
[19] Zachariasen W H 1978 *Proc. Natl. Acad. Sci. USA* **75** 1066–1067
[20] Vohra Y K and Beaver S L 1999 *J. Appl. Phys.* **85** 2451
[21] Skriver H L 1985 *Phys. Rev. B* **31**(4) 1909–1923
[22] Wills J M, Eriksson O and Boring A M 1991 *Phys. Rev. Lett.* **67**(16) 2215–2218
[23] Söderlind P, Eriksson O, Johansson B and Wills J M 1995 *Phys. Rev. B* **52**(18) 13169–13176
[24] Ravindran P, Nordström L, Ahuja R, Wills J M, Johansson B and Eriksson O 1998 *Phys. Rev. B* **57**(4) 2091–2101
[25] Richard N and Bernard S 2001 *J. Appl. Phys.* **323–324** 628–631
[26] Tian M F, Deng X, Fang Z and Dai X 2011 *Phys. Rev. B* **84**(20) 205124
[27] Zachariasen W H and Ellinger F H 1977 *Acta Crystallogr. Sec. A* **33** 155–160
[28] Ma C, Tan X, Dou Z Y, Jiang J R, Bai B, Zhu H Y, Zhang P C and Cui Q L 2017 *J. Alloy. Compd.* **712** 588 – 592
[29] Dmitriev V P, Kuznetsov A Y, Bandilet O, Bouvier P, Dubrovinsky L, Machon D and Weber H P 2004 *Phys. Rev. B* **70**(1) 014104
[30] Endo S and Fujioka N 1979 *Phys. Lett. A* **70** 475 – 476
[31] Antonova T Y, Belash I and Ponyatovskiy Y G 1981 *Phys. Met. Metall.* **51** 110–115
[32] Tsiok O and Khvostantsev L 2001 *J. Exp. Theor. Phys.* **93** 1245–1249
[33] King E, Lee J A, Harris I R and Smith T F 1970 *Phys. Rev. B* **1**(4) 1380–1381
[34] Anzellini S, Errandonea D, MacLeod S G, Botella P, Daisenberger D, De'Ath J M, Gonzalez-Platas J, Ibáñez J, McMahon M I, Munro K A, Popescu C, Ruiz-Fuertes J and Wilson C W 2018 *Phys. Rev. Materials* **2**(8) 083608 URL https://link.aps.org/doi/10.1103/PhysRevMaterials.2.083608
[35] Coleman A L, Stevenson M, McMahon M I and Macleod S G 2018 *Phys. Rev. B* **97**(14) 144107 URL https://link.aps.org/doi/10.1103/PhysRevB.97.144107
[36] Dorogokupets P I and Oganov A R 2007 *Phys. Rev. B* **75**(2) 024115
[37] Cynn, H and Baer, BJ and MacLeod, SG and Evans, WJ and Lipp, MJ and Klepeis, JP and Jenei, Z and Chen, JY and Catalli, K and Popov, D and Park, CY 2012 Comparison of the existing internally consistent pressure scales at high pressures and high temperatures *APS Meeting Abstracts*
[38] Dorogokupets P I and Dewaele A 2007 *High Press. Res.* **27** 431–446
[39] Hammersley A P, Svensson S O, Hanfland M, Fitch A N and Hausermann D 1996 *High Press. Res.* **14** 235–248
[40] Petrícek V, Dusek M and Palatinus L 2006 *The Crystallographic Computing System JANA2006* Institute of Physics, Prague
[41] Singh A K and Takemura K 2001 *J. Appl. Phys.* **90** 3269–3275
[42] Ma C, Dou Z Y, Zhu H Y, Fu G Y, Tan X, Bai B, Zhang P C and Cui Q L 2016 *Chinese Physics B* **25** 046401